

# Metal–Bis(2-picolyl)amine Complexes as State 1(T) Inhibitors of Activated Ras Protein\*\*

Ina C. Rosnizeck, Michael Spoerner, Tobias Harsch, Sandra Kreitner, Daniel Filchtinski, Christian Herrmann, Daniel Engel, Burkhard König, and Hans Robert Kalbitzer\*

The small guanine nucleotide binding (GNB) protein Ras is a central component in cellular signaling networks controlling proliferation, differentiation, and apoptosis. Alternating between an inactive GDP- and an active GTP-bound form, Ras acts as molecular switch, which is regulated by guanine nucleotide exchange factors (GEFs) and GTPase-activating proteins (GAPs) (see, for example, Ref. [1]). Ras with GTP bound strongly interacts with effectors such as Raf kinase, RalGDS, and PI3 kinase that transmit the incoming activation signal to downstream targets.<sup>[2]</sup> <sup>31</sup>P NMR spectroscopy was used to identify two distinct conformational states in Ras when a nucleoside triphosphate (T) is bound, called state 1(T) and state 2(T).<sup>[3]</sup> These states were first defined by the spectroscopic properties: in state 1(T) the <sup>31</sup>P NMR resonance lines of the  $\alpha$ - and  $\gamma$ -phosphate groups are shifted downfield relative to those corresponding to state 2(T).<sup>[4]</sup> These states are in dynamic equilibrium, with exchange rates on the millisecond timescale at room temperature. Ras in state 1(T) has a more than 2 orders of magnitude lower affinity for effectors than Ras in state 2(T).<sup>[4,5]</sup> The affinity of the two states for Raf was estimated as 7  $\mu$ M and 0.012  $\mu$ M, respectively, at 283 K.<sup>[4b]</sup> In contrast, the guanine nucleotide exchange factor Sos binds preferentially to state 1(T).<sup>[6]</sup> State 2(T) becomes stabilized when Ras is complexed to the Ras-binding domains (RBDs) of its effectors such as Raf kinase, RalGDS, AF-6, and Byr2,<sup>[3,7]</sup> and is consequently also

referred to as the effector-binding state. For wild-type (wt) H-Ras(1–166) the equilibrium constant  $K_{12}$  for the two states is 11.3 in the presence of its natural ligand GTP.<sup>[8]</sup> Partial loss-of-function mutants, such as Ras(T35A) and Ras(T35S), complexed to  $Mg^{2+}$ -GppNHp (GppNHp = guanosine-5'-( $\beta$ , $\gamma$ -imino)triphosphate) activate only a subset of the known Ras effectors and predominantly exist in the weak effector-binding conformational state 1(T).<sup>[4b]</sup> In cancer research Ras represents a target of high interest owing to its critical involvement in about 30% of all human malignancies.<sup>[9]</sup> Oncogenic Ras cannot be switched off by either by its intrinsic GTPase activity or by GAPs, leading to uncontrolled cell growth and thus to tumor formation.

To date, there have been extensive efforts to find small compounds that interrupt the Ras-mediated signal transduction with Ras as the target. Different strategies have been followed: 1) targeting Ras activation by inhibition of nucleotide exchange,<sup>[10]</sup> and 2) increasing the GTPase activity of oncogenic Ras mutants thus deactivating Ras;<sup>[11]</sup> however, suitable compounds have not been found yet. A further strategy is 3) the inhibition of the Ras–effector interaction by small compounds<sup>[12]</sup> or peptides.<sup>[13]</sup> For the latter approach selective stabilization of the weak effector-binding state 1(T) by small compounds represents a promising novel strategy for the inhibition of oncogenic Ras signaling.<sup>[14]</sup> In fact,  $M^{2+}$ -cyclens and their peptide conjugates recognize exclusively the conformational state 1(T).<sup>[15]</sup> This small ligand is directly coordinated to the  $\gamma$ -phosphate of the bound nucleotide.<sup>[16]</sup>


Ligands binding to the  $\gamma$ -phosphate group of the nucleotide in the nucleotide-binding cleft are natural candidates for stabilizing state 1(T) since the region around the  $\gamma$ -phosphate is accessible only in state 1(T). However, since the general mechanism of action is fundamentally an allosteric mechanism, the ligand-binding site does not have to be located in the active center cleft or the effector interaction site. Herein we report an alternative class of state 1(T) stabilizers that interact with Ras- $Mg^{2+}$ -GTP outside the nucleotide-binding site. Lead compounds are metal(II)-bis(2-picolyl)amines ( $M^{2+}$ -BPAs)<sup>[17]</sup> (Figure 1a) that also influence the equilibrium between states 1 and 2 in the desired way.<sup>[18]</sup>

State 1(T) inhibitors can be detected quite easily by analyzing the <sup>31</sup>P NMR signals representing conformational states 1 and 2 of Ras- $Mg^{2+}$ -GppNHp, whose integrals are a direct measure of the population of the corresponding state. In the wild-type protein two sets of resonances can be found for the  $\alpha$ - and  $\gamma$ -phosphate groups, respectively, when the protein is complexed to the GTP analogue GppNHp.<sup>[3,5a]</sup> In the presence of  $Zn^{2+}$ -BPA the peak areas of the signals for the  $\alpha$ - and  $\gamma$ -phosphate groups characteristic for conforma-

[\*] Dr. I. C. Rosnizeck,<sup>[†]</sup> Priv.-Doz. Dr. M. Spoerner,<sup>[†]</sup> T. Harsch, Dr. S. Kreitner, Prof. Dr. Dr. H. R. Kalbitzer  
Institut für Biophysik und Physikalische Biochemie  
Universität Regensburg  
Universitätsstrasse 31, 93053 Regensburg (Germany)  
E-mail: hans-robert.kalbitzer@biologie.uni-regensburg.de  
Dr. D. Filchtinski, Prof. Dr. C. Herrmann  
Institut für Physikalische Chemie  
Ruhr-Universität Bochum (Germany)  
Dr. D. Engel, Prof. Dr. B. König  
Institut für Organische Chemie  
Universität Regensburg (Germany)

[†] I.C.R. and M.S. contributed equally to this work.

[\*\*] This work was supported financially by the Deutsche Forschungsgemeinschaft, the Fonds der Chemischen Industrie, and the Volkswagenstiftung. We thank Georg Discherl and Florian Schmidt for the synthesis of the  $M^{2+}$ -BPA complexes.

 Supporting information for this article (including details of the protein purification, NMR and fluorescence spectroscopy, the evaluation of the chemical shift changes and the paramagnetic relaxation enhancement induced by ligand binding, and the structure calculation) are available on the WWW under <http://dx.doi.org/10.1002/anie.201204148>.

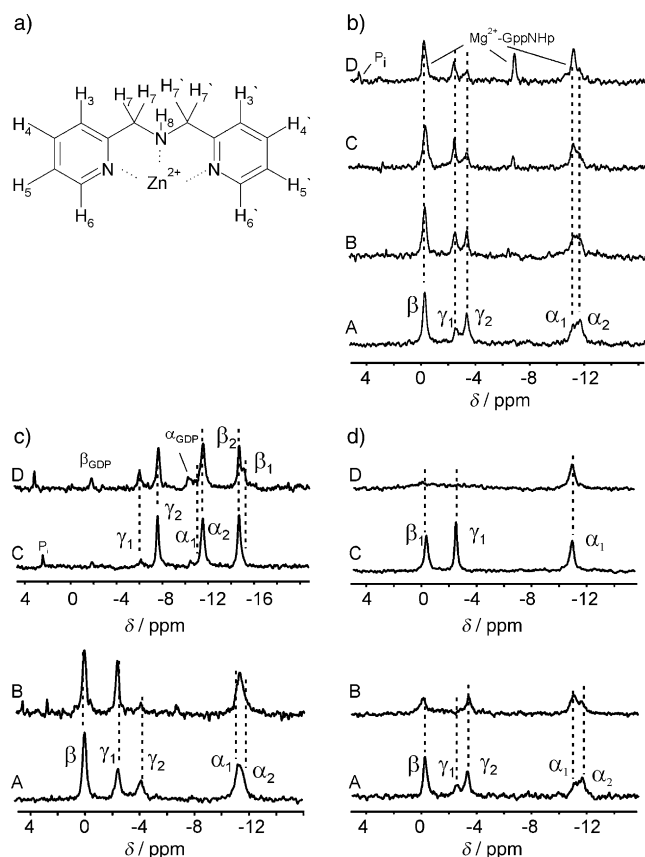


**Figure 1.** Influence of  $M^{2+}$ -BPA on the dynamic equilibrium of active Ras complexes. a) Molecular structure of zinc(II) bis(2-picolyl)amine. b)  $^{31}\text{P}$  NMR spectra of 0.4 mM Ras(wt)· $\text{Mg}^{2+}$ -GppNHp in the absence (A) and in the presence of  $\text{Zn}^{2+}$ -BPA with a concentration of 3 mM (B), 5.6 mM (C), and 9 mM (D). c) Influence of  $\text{Zn}^{2+}$ -BPA on Ras(G12V).  $\text{P}_i$  = inorganic phosphate.  $^{31}\text{P}$  NMR spectra of 0.6 mM Ras(G12V)· $\text{Mg}^{2+}$ -GppNHp (A) and 0.6 mM Ras(G12V)· $\text{Mg}^{2+}$ -GTP (C) in the absence (A, C) and presence of 5.3 mM (B) and 11 mM  $\text{Zn}^{2+}$ -BPA (D), respectively. d) Influence of  $\text{Cu}^{2+}$ -BPA on Ras· $\text{Mg}^{2+}$ -GppNHp.  $^{31}\text{P}$  NMR spectra of 0.6 mM Ras(wt)· $\text{Mg}^{2+}$ -GppNHp in the absence (A) and in the presence of 4.3 mM  $\text{Cu}^{2+}$ -BPA (B). 0.7 mM Ras(T35A)· $\text{Mg}^{2+}$ -GppNHp in the absence (C) and in the presence of 5 mM  $\text{Cu}^{2+}$ -BPA (D). All measurements were performed at 278 K. Buffer: 40 mM Tris/HCl pH 7.4, 10 mM  $\text{MgCl}_2$ , 2 mM DTE, 0.2 mM DSS, and 5%  $\text{D}_2\text{O}$ .  $\alpha_1$ ,  $\beta_1$ ,  $\gamma_1$ ,  $\alpha_2$ ,  $\beta_2$ ,  $\gamma_2$ : resonances of the  $\alpha$ -,  $\beta$ -, and  $\gamma$ -phosphate groups in state 1 and state 2, respectively. DTE = dithioerythritol, DSS = 2,2-dimethyl-2-silapentane-5-sulfonate, Tris = tris-(hydroxymethyl)aminomethane.

tional state 1(T) in the wild-type protein increase, while those representing conformational state 2(T) decrease at the same time (Figure 1 b). The  $^{31}\text{P}$  chemical shifts of the protein-bound nucleotide do not change much when  $\text{Zn}^{2+}$ -BPA is bound to the protein, whereas the interaction of  $\text{Zn}^{2+}$ -BPA with the free  $\text{Mg}^{2+}$ -GppNHp leads to large changes in the chemical shifts. At the same ligand concentration the resonance lines of the  $\alpha$ - and  $\beta$ -phosphate groups show upfield chemical shifts of more than 1 ppm and a downfield shift of approximately 0.8 ppm for the  $\gamma$ -phosphate group (Table S1 in the Supporting Information). These shifts are mainly due to the interaction of the  $\text{Zn}^{2+}$  ion with the phosphate groups. Since effects of similar magnitude would be expected for the protein-

bound nucleotide if it would directly interact with  $\text{Zn}^{2+}$ -BPA, the metal ion is most probably not coordinated directly to one of the phosphate groups in the protein complex. As an additional effect of  $\text{Zn}^{2+}$ -BPA binding, at a  $\text{Zn}^{2+}$ -BPA concentration of 6 mM the signals representing free  $\text{Mg}^{2+}$ -GppNHp in complex with  $\text{Zn}^{2+}$ -BPA (Table S1) become visible (Figure 1 b) and simultaneously nucleotide-free Ras precipitates (as revealed by SDS-PAGE analysis). At the highest  $\text{Zn}^{2+}$ -BPA concentration used (10 mM) approximately 50 % of the total nucleotide is released.

By saturation transfer difference (STD) NMR spectroscopy<sup>[19]</sup> we can determine the affinity of  $\text{Zn}^{2+}$ -BPA (Figure S1 a in the Supporting Information) to activated Ras. For the mutant Ras(T35A)· $\text{Mg}^{2+}$ -GppNHp, which exists predominantly in the weak effector-binding state 1(T) of active Ras,<sup>[4b]</sup> we obtain an apparent dissociation constant of  $(2.1 \pm 0.3)$  mM (Figure S1 c).

A shift of the equilibrium towards the weak effector-binding state by  $\text{Zn}^{2+}$ -BPA is also found in the complex of the oncogenic mutant Ras(G12V) with the GTP analogue GppNHp (Figure 1 c, bottom). Since Ras(G12V)· $\text{Mg}^{2+}$ -GTP exhibits a very slow hydrolysis rate of  $0.002 \text{ min}^{-1}$  at  $37^\circ\text{C}$ ,<sup>[8]</sup> investigations of this mutant bound to true substrate GTP are possible at low temperature. The set of phosphorus resonances of the bound nucleotide predominantly observed in the  $^{31}\text{P}$  NMR spectrum of Ras(G12V)· $\text{Mg}^{2+}$ -GTP (Figure 1 c, top) was assigned earlier to conformational state 2(T).<sup>[8]</sup> In the presence of  $\text{Zn}^{2+}$ -BPA a second set of resonances is observed for the  $\gamma$ - and  $\beta$ -phosphate groups (Figure 1 c). The chemical shift values correspond to conformational state 1(T) that is also detectable in the spectra of wild-type Ras· $\text{Mg}^{2+}$ -GTP (Table S1 in the Supporting Information).

For obtaining more quantitative structural information we used the paramagnetic  $\text{Cu}^{2+}$  derivative of BPA. In contrast to the diamagnetic  $\text{Zn}^{2+}$  ion it induces a distance-dependent  $T_2$  relaxation (line broadening) of nearby nuclei because of the strong magnetic moment of its unpaired electrons. In wild-type Ras· $\text{Mg}^{2+}$ -GppNHp the lines corresponding to the phosphate groups in state 1(T) are strongly broadened (Figure 1 d), whereas the resonances corresponding to state 2(T) are virtually unchanged. This indicates that  $\text{Cu}^{2+}$ -BPA binds exclusively to state 1(T). The  $\alpha$ -phosphate resonance is still observable in state 1(T) at a concentration ratio  $\text{Cu}^{2+}$ -BPA/protein of 8:1 (i.e. 4.3 mM) and its integral is increased relative to that of state 2(T). This indicates that  $\text{Cu}^{2+}$ -BPA binding shifts the equilibrium towards the weak effector-binding state in the wild-type protein. In the state 1(T) mutant Ras(T35A)· $\text{Mg}^{2+}$ -GppNHp (Figure 1 d) the line-broadening effect can be observed very clearly, as in the wild-type protein the  $\beta$ - and  $\gamma$ -phosphate signals are broadened to a greater extent than the signals of the  $\alpha$ -phosphate group. At a fourfold molar excess of  $\text{Cu}^{2+}$ -BPA the linewidth of the  $\gamma$ -phosphate signal assigned to state 1 is already 563 Hz compared to a linewidth of 71 Hz in the absence of the compound, and the signal is no longer detectable in the presence of 5 mM  $\text{Cu}^{2+}$ -BPA (Figure 1 d).

The  $^{31}\text{P}$  NMR data indicate that  $M^{2+}$ -BPA is not coordinated directly to the phosphate groups since the typical shifts induced by direct binding are not observed. Additional

information on the binding site can be obtained from the paramagnetic relaxation enhancement by  $\text{Cu}^{2+}$ -BPA detected in the  $[^1\text{H}, ^{15}\text{N}]$  HSQC spectra of Ras-(T35A)· $\text{Mg}^{2+}$ ·GppNHp. The diamagnetic ligand  $\text{Zn}^{2+}$ -BPA causes analogous chemical shift changes  $\Delta\delta_{\text{combined}} > \sigma_0^{\text{corr}}$  in the titration experiments (Figure S2a in the Supporting Information). The strongest chemical shift changes are observed for residues Asp38, Ser39, and Tyr40 as well as for the C-terminal residues Ile163, Gln165, and His166. Additional large changes can be found for Ile139, which is in close proximity to the C-terminal end, and for Lys147, which is close to nucleotide binding motif G1. Phe28, which is part of the G1 motif itself and forms strong hydrophobic interaction with the guanine base, is also affected significantly together with residues in its neighbourhood. Table S2 summarizes the results of the  $[^1\text{H}, ^{15}\text{N}]$  HSQC titration experiments on Ras with  $\text{M}^{2+}$ -BPA. When these data are projected onto the surface of the structure of Ras(T35S)· $\text{Mg}^{2+}$ ·GppNHp, which was solved earlier by NMR spectroscopy,<sup>[20]</sup> two distinct binding sites are revealed. One binding site (Figure S2b, C and D) is located at the C-terminal end of Ras and at loop L7. A similar site was also found for  $\text{M}^{2+}$ -cyclen both by NMR spectroscopy and by X-ray crystallography.<sup>[16]</sup> The second site (Figure S2b, A and B) is located close to the active center and is presumably responsible for the stabilization of conformational state 1(T). However, its position determined from the chemical shift and paramagnetic relaxation perturbation studies differs from the binding site obtained for  $\text{M}^{2+}$ -cyclen. Here,  $\text{M}^{2+}$ -BPA is most probably located outside of the nucleotide-binding pocket close to Asp38, Ser39, and Tyr40.

The binding site for  $\text{M}^{2+}$ -BPA close to the C-terminus shows the strongest paramagnetic relaxation enhancement and diamagnetic shift changes involving residues Gln165 and His166. The metal ion of  $\text{Zn}^{2+}$ -cyclen is directly coordinated to the imidazole ring of His166. Therefore, the coordination of the metal ion of  $\text{M}^{2+}$ -BPA to the imidazole ring in His166 is probably defining ligand-binding site 2. In the mutant Ras(T35A/H166A) the second binding site for  $\text{M}^{2+}$ -BPA and  $\text{M}^{2+}$ -cyclen should be destroyed. In line with the expectation, STD measurements show that this mutant still binds the ligands. In the soft $[^1\text{H}, ^{15}\text{N}]$  HMQC spectra, clear chemical shift changes at site 1 are still observed after ligand binding but the effects concerning the C-terminal residues have almost disappeared (Figure S3 and S4 in the Supporting Information). In the main binding site 1 the chemical shift pattern differs clearly between  $\text{Zn}^{2+}$ -cyclen and  $\text{Zn}^{2+}$ -BPA (Figure S3). The addition of  $\text{Cu}^{2+}$ -BPA leads to the same line broadening in the  $^{31}\text{P}$  NMR spectra of Ras(T35A/H166A)· $\text{Mg}^{2+}$ ·GppNHp (Figure 2a) as those observed for Ras(T35A)· $\text{Mg}^{2+}$ ·GppNHp (Figure S2c). It shows that an interaction with the C-terminal binding site is not the cause for the stabilization of state 1(T). If  $\text{Cu}^{2+}$ -BPA would bind at the same site as the diamagnetic  $\text{Zn}^{2+}$ -cyclen, it should be released when  $\text{Zn}^{2+}$ -cyclen is added in high concentrations. This is clearly not the case (Figure 2) indicating that the binding site of  $\text{M}^{2+}$ -BPA is located outside the nucleotide-binding cleft.

The final goal of the drug design is the inhibition of the oncogenic activated Ras mutants. A prominent group of

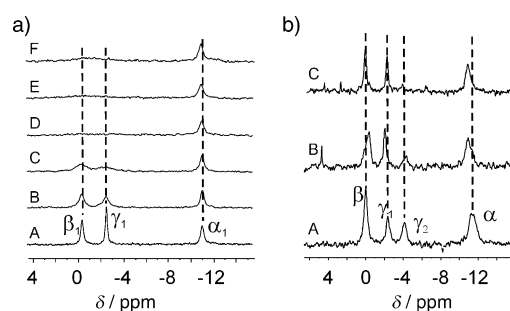


**Figure 2.** Titration of Ras(T35A/H166A) with  $\text{Cu}^{2+}$ -BPA and  $\text{Zn}^{2+}$ -cyclen and titration of Ras(G12V) with  $\text{Zn}^{2+}$ -cyclen and with  $\text{Zn}^{2+}$ -BPA. a) The sample initially contained 2.1 mM Ras(T35A/H166A)· $\text{Mg}^{2+}$ ·GppNHp.  $^{31}\text{P}$  NMR spectra of the sample A) before addition of a ligand and after addition of B) 1.6 mM  $\text{Cu}^{2+}$ -BPA, C) 3.6 mM  $\text{Cu}^{2+}$ -BPA, and D) 14.8 mM  $\text{Cu}^{2+}$ -BPA. Spectra from a sample containing E) 14.6 mM  $\text{Cu}^{2+}$ -BPA and 10 mM  $\text{Zn}^{2+}$ -cyclen, and F) 14.4 mM  $\text{Cu}^{2+}$ -BPA and 22.5 mM  $\text{Zn}^{2+}$ -cyclen. b) Stabilization of state 1(T) in the oncogenic mutant Ras(G12V) by  $\text{Zn}^{2+}$ -BPA and  $\text{Zn}^{2+}$ -cyclen.  $^{31}\text{P}$  NMR spectra of A) initially 0.6 mM Ras-(G12V)· $\text{Mg}^{2+}$ ·GppNHp, B) sample of (A) in the presence of 24 mM  $\text{Zn}^{2+}$ -cyclen, and C) in the presence of 5.3 mM  $\text{Zn}^{2+}$ -BPA. All spectra were recorded at 278 K. Buffer: 50 mM Tris/HCl pH 7.4, 10 mM  $\text{MgCl}_2$ , 10%  $\text{D}_2\text{O}$ , and 0.1 mM DSS.

oncogenic mutants have point mutations at position 12. Therefore, we studied the interaction of  $\text{Zn}^{2+}$ -BPA and  $\text{Zn}^{2+}$ -cyclen with the Ras mutant G12V. Figure 2b presents the results: both compounds are able to stabilize state 1(T) but the  $\text{Zn}^{2+}$ -BPA described here is clearly more powerful than the cyclen derivative. Whereas  $\text{Zn}^{2+}$ -BPA is able to completely shift the equilibrium to state 1(T) at a concentration of 5 mM, for  $\text{Zn}^{2+}$ -cyclen even at a 5 times higher concentration state 1(T) is not completely selected. This is probably due to steric hindrance by the valine side chain close to the  $\gamma$ -phosphate. This side chain does not play a role in  $\text{Zn}^{2+}$ -BPA binding since this ligand binds outside the active center.

The experimental data (Table S2 in the Supporting Information) can be used to obtain a structural model of the complex of  $\text{Zn}^{2+}$ -BPA to Ras· $\text{Mg}^{2+}$ ·GppNHp. Since we have shown above that  $\text{Zn}^{2+}$ -BPA bound to site 1 but not to site 2 can shift the equilibrium to state 1(T), only the modeling of the complex of  $\text{Zn}^{2+}$ -BPA bound to site 1 of Ras· $\text{Mg}^{2+}$ ·GppNHp in state 1(T) is pharmaceutically relevant. Since we have shown that  $\text{Zn}^{2+}$ -BPA can also bind to Ras complexed with  $\text{Zn}^{2+}$ -cyclen, we used the previously determined structure of the Ras· $\text{Zn}^{2+}$ -cyclen complex in ligand docking studies.<sup>[16]</sup> HADDOCK<sup>[21]</sup> was used for the calculation of complex structures on the basis of the chemical shift perturbation data (ambiguous restraints) from  $\text{Zn}^{2+}$ -BPA titration experiments and the paramagnetic relaxation enhancement data (unambiguous restraints) from  $\text{Cu}^{2+}$ -BPA titration experiments (Table S2). The obtained structures with high HADDOCK scores are all quite similar. The structure of the complex with the highest score is depicted in Figure 3. In this structure  $\text{Zn}^{2+}$ -BPA is bound in a negatively charged pocket of the state 1(T) structure with the  $\text{Zn}^{2+}$  ion bound to the negatively charged carboxylate anion in the side chain of Asp38. The methylene groups and one of the aromatic rings

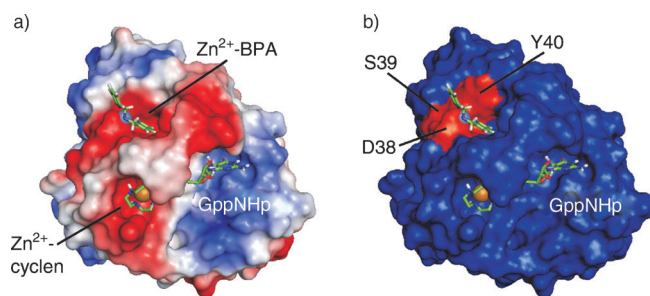


**Figure 3.** Ligand binding site of  $M^{2+}$ -BPA on Ras-GppNHp. Structure of the complex Ras(T35A)· $Mg^{2+}$ ·GppNHp· $Zn^{2+}$ -cyclen with  $Zn^{2+}$ -BPA as derived from molecular dynamics calculations with HADDOCK<sup>[21]</sup> using the restraints obtained by chemical shift perturbations and paramagnetic relaxation enhancements in  $^{31}P$  NMR and  $[^1H, ^{15}N]$  HSQC titration experiments (Figure S2; Table S2). Structure shown a) with the electrostatic surface of Ras and b) with Ras residues highlighted that contribute to the surface and show the strongest effects, namely residues 38–40 (Table S2).

are in close contact with the surface of the protein as predicted by the STD experiments (Figure S1). One should mention here that this binding site corresponds also to one of the hot spots predicted recently.<sup>[12c,d]</sup>

As we have shown above,  $Zn^{2+}$ -BPA stabilizes the weak effector-binding state 1(T). Therefore, it can be considered as a lead structure for the allosteric inhibition of Ras signaling by effector binding. As shown by  $^{31}P$  NMR spectroscopy<sup>[4b]</sup> in the state 1(T) mutant Ras(T35S)· $Mg^{2+}$ ·GppNHp the dynamic equilibrium can be shifted towards the strong effector-binding state 2(T) by addition of Raf-RBD (Figure 4a). As expected, the equilibrium can be shifted back towards the weak effector-binding state 1(T) by addition of  $Zn^{2+}$ -BPA: The signals representing conformational state 1(T) increase after addition of  $Zn^{2+}$ -BPA (Figure 4a).

Additionally, stopped-flow measurements have been performed with wild-type Ras loaded with the fluorescently labeled nonhydrolyzable GTP analogue mantGppNHp and Raf-RBD in the absence and presence of  $Zn^{2+}$ -BPA. As one can see very clearly in Figure 4b the observed rate constants for the association between Ras and Raf-RBD are substantially decreased in the presence of  $Zn^{2+}$ -BPA. In the absence of  $Zn^{2+}$ -BPA a typical nonlinear dependence of the apparent “on” rate  $k_{obs}$  on the Raf-RBD binding is observed (Figure 4b) indicating a two-step binding process.<sup>[4b]</sup> In the presence of  $Zn^{2+}$ -BPA the observed “on” rate is substantially smaller and shows a typical linear concentration dependence, as observed earlier for the state 1(T) mutant Ras(T35A). This indicates that it is not possible to shift the equilibrium back towards the strong effector-binding conformation 2(T) by addition of Raf-RBD in the concentration range studied.

The inhibitory binding site for  $Zn^{2+}$ -cyclen is clearly defined by the coordination of the metal ion with the  $\gamma$ -phosphate of the nucleoside triphosphate. In line with the coordination of  $Zn^{2+}$ -cyclen with the  $\gamma$ -phosphate an interaction with GDP lacking a  $\gamma$ -phosphate group was not observed.<sup>[16]</sup> However, all evidence indicates that interaction site of  $Zn^{2+}$ -BPA is located outside of the nucleotide binding cleft close to a patch formed by amino acids at positions 38 to 40 and 53 to 58. In line with this model our  $^{31}P$  NMR data

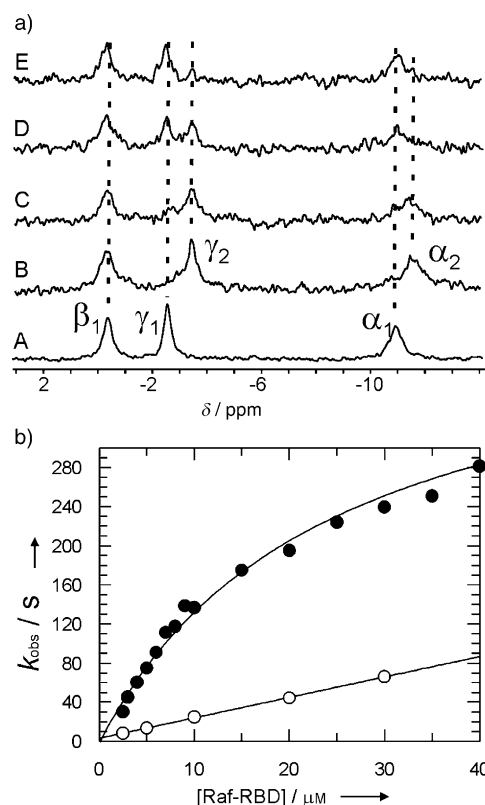


**Figure 4.** Effect of  $Zn^{2+}$ -BPA on Ras-effector interaction. a) Displacement of Raf-RBD from Ras(T35S)· $Mg^{2+}$ ·GppNHp by  $Zn^{2+}$ -BPA. The sample initially contained 0.8 mM Ras(T35S)· $Mg^{2+}$ ·GppNHp in 40 mM Tris/HCl pH 7.4, 10 mM  $MgCl_2$ , 2 mM DTE, 0.2 mM DSS and 5%  $D_2O$ . a) The  $^{31}P$  NMR spectra were recorded in the absence of Raf-RBD (A), 0.6 mM Ras(T35S)· $Mg^{2+}$ ·GppNHp presence of a 0.9 mM Raf-RBD (B). Subsequently,  $Zn^{2+}$ -BPA was added to the sample shown in (B) with concentration of 2.4 mM (C), 4.5 mM (D), and 6.4 mM (E), respectively. All spectra were recorded at 278 K. b) Kinetics of the association between wildtype Ras-GppNHp and Raf-RBD in the absence and presence of  $Zn^{2+}$ -BPA. The observed apparent rate constants  $k_{obs}$  are plotted against the Raf-RBD concentration in the absence (black dots) and in the presence (white dots) of 10 mM  $Zn^{2+}$ -BPA. The measurements were performed at 283 K and 15 mM Hepes/NaOH pH 7.5, 125 mM NaCl, 5 mM  $MgCl_2$ . Hepes = 4-(2-hydroxyethyl)-1-piperazine-ethanesulfonic acid.

further indicate that  $M^{2+}$ -BPA, in contrast to the  $M^{2+}$ -cyclens, also can interact with Ras in the GDP-bound “off” state (Figure S5 and Table S3 in the Supporting Information).

The existence of two different, locally separated inhibitory binding sites for these two lead structures has practical consequences. As we have shown experimentally, both  $Zn^{2+}$ -cyclen and  $Zn^{2+}$ -BPA can bind simultaneously and therefore probably mutually increase their effect. In principle, the two fragments could be linked chemically thus enhancing their affinity as it is typically done in fragment-based drug design. Such a binding is also in agreement with our structural model (Figure 2). The advantage of compounds that recognize the  $Zn^{2+}$ -cyclen binding site is that in principle they could also recognize oncogenic mutations at positions 12, 13, and 61 by a direct interaction with the side chains of the mutated residues. However, a steric conflict with the side chains of the mutated amino acids or a local conformational change can



also cause a lower affinity for the oncogenic mutants as a negative side effect. This applies for Ras(G12V), which has a lower affinity for Zn<sup>2+</sup>-cyclen than the wild-type protein. In contrast, the binding position of Zn<sup>2+</sup>-BPA is not affected by this mutation and the latter compound can bind without any difficulty. (Figure 3). Therefore, Zn<sup>2+</sup>-BPA binds significantly stronger to Ras(G12V) than Zn<sup>2+</sup>-cyclen.

Both Zn<sup>2+</sup>-BPA and Zn<sup>2+</sup>-cyclen stabilize the Sos-interacting state 1(T).<sup>[6]</sup> As a main effect they weaken the interaction with effectors since these prefer state 2(T). In this way they also slow down the intrinsic (and possibly the GAP-catalyzed) GTPase activity that requires the structural arrangement of state 2(T) around the  $\gamma$ -phosphate.<sup>[8]</sup> For permanently activated oncogenic Ras mutants this would not play a negative role as long as the effector interaction is disturbed. A shift of the equilibrium to state 1(T) should also influence the nucleotide-exchange reaction by influencing the nucleotide exchange in the absence of Sos. This is indeed experimentally observed for Zn<sup>2+</sup>-BPA (see above) and was also observed for Zn<sup>2+</sup>-cyclen (unpublished results). The equilibrium is shifted towards the nucleotide-free state and GTP is released. After the binding of the two state 1(T) inhibitors one would also expect a stronger interaction with SOS,<sup>[20]</sup> an effect that is worth examining in detail. Zn<sup>2+</sup>-BPA binds also to Ras-Mg<sup>2+</sup>-GDP. This could mean that in analogy, the binding of Zn<sup>2+</sup>-BPA to Ras-Mg<sup>2+</sup>-GDP could stabilize the corresponding state 1(D), an interesting conjecture yet to be verified experimentally.

In summary, we can show that both state 1(T) inhibitors suppress Ras-effector interactions in vitro, although they have completely different interactions sites. The control of the conformational equilibrium between Ras substates with small organic ligands like Zn<sup>2+</sup>-cyclen and Zn<sup>2+</sup>-BPA is based on a mechanism that differs from that of classical competitive inhibitors. Of course, the site 1(T) inhibitors discussed here can only serve as leads for the development of compounds with considerably higher affinity required for medical applications.

Received: May 28, 2012

Published online: September 20, 2012

**Keywords:** conformational dynamics · drug design · Ras protein · signal transduction

- [1] A. Wittinghofer, H. Waldmann, *Angew. Chem.* **2000**, *112*, 4360–4383; *Angew. Chem. Int. Ed.* **2000**, *39*, 4192–4214.
- [2] C. Herrmann, *Curr. Opin. Struct. Biol.* **2003**, *13*, 122–129.
- [3] M. Geyer, T. Schweins, C. Herrmann, T. Prisner, A. Wittinghofer, H. R. Kalbitzer, *Biochemistry* **1996**, *35*, 10308–10320.
- [4] a) M. Spoerner, A. Wittinghofer, H. R. Kalbitzer, *FEBS Lett.* **2004**, *578*, 305–310; b) M. Spoerner, C. Herrmann, I. R. Vetter, H. R. Kalbitzer, A. Wittinghofer, *Proc. Natl. Acad. Sci. USA* **2001**, *98*, 4944–4949.
- [5] a) M. Spoerner, A. Nuehs, P. Ganser, C. Herrmann, A. Wittinghofer, H. R. Kalbitzer, *Biochemistry* **2005**, *44*, 2225–2236; b) M. Spoerner, A. Nuehs, C. Herrmann, G. Steiner, H. R. Kalbitzer, *FEBS J.* **2007**, *274*, 1419–1433.
- [6] H. R. Kalbitzer, M. Spoerner, P. Ganser, C. Hosza, W. Kremer, *J. Am. Chem. Soc.* **2009**, *131*, 16714–16719.
- [7] a) M. Geyer, C. Herrmann, S. Wohlgemuth, A. Wittinghofer, H. R. Kalbitzer, *Nat. Struct. Biol.* **1997**, *4*, 694–699; b) T. Linnemann, M. Geyer, B. K. Jaitner, C. Block, H. R. Kalbitzer, A. Wittinghofer, C. Herrmann, *J. Biol. Chem.* **1999**, *274*, 13556–13562; c) W. Gronwald, F. Huber, P. Grünwald, M. Spörner, S. Wohlgemuth, C. Herrmann, A. Wittinghofer, H. R. Kalbitzer, *Structure* **2001**, *9*, 1029–1041.
- [8] M. Spoerner, C. Hosza, J. A. Poetzl, K. Reiss, P. Ganser, M. Geyer, H. R. Kalbitzer, *J. Biol. Chem.* **2010**, *285*, 39768–39778.
- [9] a) J. L. Bos, *Cancer Res.* **1989**, *49*, 4682–4689; b) A. T. Baines, D. Xu, C. J. Der, *Future Med. Chem.* **2011**, *3*, 1787–808; c) B. B. Friday, A. A. Adjei, *Biochim. Biophys. Acta Rev. Cancer* **2005**, *1756*, 127–144.
- [10] a) A. Palmioli, E. Sacco, S. Abraham, C. J. Thomas, A. Di Domizio, L. De Gioia, V. Gaponenko, M. Vanoni, F. Peri, *Bioorg. Med. Chem. Lett.* **2009**, *19*, 4217–4222; b) S. Colombo, A. Palmioli, C. Airoidi, R. Tisi, S. Fantinato, S. Olivieri, L. De Gioia, E. Martegani, F. Peri, *Curr. Cancer Drug Targets* **2010**, *10*, 192–199; c) E. Sacco, et al., *Biotechnol. Adv.* **2012**, *30*, 233–243; d) C. Müller, et al., *ChemMedChem* **2009**, *4*, 524–528; e) T. Maurer, et al., *Proc. Natl. Acad. Sci. USA* **2012**, *109*, 5299–5304; f) Q. Sun, J. P. Burke, J. Phan, M. C. J. Burns, E. T. Olejniczak, A. G. Waterson, T. Lee, O. W. Rossanese, S. W. Fesik, *Angew. Chem.* **2012**, *124*, 6244–6247; *Angew. Chem. Int. Ed.* **2012**, *51*, 6140–6143.
- [11] a) T. Zor, M. Bar-Yaacov, S. Elgavish, B. Shaanan, Z. Selinger, *Eur. J. Biochem.* **1997**, *249*, 330–336; b) M. R. Ahmadian, T. Zor, D. Vogt, W. Kabsch, Z. Selinger, A. Wittinghofer, K. Scheffzek, *Proc. Natl. Acad. Sci. USA* **1999**, *96*, 7065–7070; c) R. Gail, B. Costisella, M. R. Ahmadian, A. Wittinghofer, *ChemBioChem* **2001**, *2*, 570–575; d) L. Soullère, C. Aldrich, O. Daumke, R. Gail, L. Kissau, A. Wittinghofer, H. Waldmann, *ChemBioChem* **2004**, *5*, 1448–1453.
- [12] a) O. Müller, E. Gourzoulidou, M. Carpintero, I. M. Karaguni, A. Langerak, C. Herrmann, T. Mörröy, L. Klein-Hitpass, H. Waldmann, *Angew. Chem.* **2004**, *116*, 456–460; *Angew. Chem. Int. Ed.* **2004**, *43*, 450–454; b) H. Waldmann, I. M. Karaguni, M. Carpintero, E. Gourzoulidou, C. Herrmann, C. Brockmann, H. Oschkinat, O. Müller, *Angew. Chem.* **2004**, *116*, 460–464; *Angew. Chem. Int. Ed.* **2004**, *43*, 454–458; c) B. J. Grant, S. Lukman, H. J. Hocker, J. Sayyah, J. H. Brown, J. A. McCammon, A. A. Gorfe, *PLoS One* **2011**, *6*, e25711; d) G. Buhrman, et al., *J. Mol. Biol.* **2011**, *413*, 773–789.
- [13] a) F. Barnard, H. Sun, L. Baker, M. S. Marshall, *Biochem. Biophys. Res. Commun.* **1998**, *247*, 176–180; b) P. C. Gareiss, A. R. Schneekloth, M. J. Salcius, S. Y. Seo, C. M. Crews, *ChemBioChem* **2010**, *11*, 517–522.
- [14] H. R. Kalbitzer, B. Koenig, PCT Int. Appl. 14 pp. WO 2004006934 A2 20040122, **2004** [CAN 140:122769; AN 2004:60322].
- [15] a) M. Spoerner, T. Graf, B. König, H. R. Kalbitzer, *Biochem. Biophys. Res. Commun.* **2005**, *334*, 709–713; b) F. Schmidt, I. C. Rosnizeck, M. Spoerner, H. R. Kalbitzer, B. König, *Inorg. Chim. Acta* **2011**, *365*, 38–48.
- [16] I. C. Rosnizeck, et al., *Angew. Chem.* **2010**, *122*, 3918–3922; *Angew. Chem. Int. Ed.* **2010**, *49*, 3830–3833.
- [17] M. Kruppa, B. König, *Chem. Rev.* **2006**, *106*, 3520–3560.
- [18] I. C. Rosnizeck, Ph.D. thesis, **2010**, University of Regensburg, Germany.
- [19] M. Mayer, B. Meyer, *Angew. Chem.* **1999**, *111*, 1902–1906; *Angew. Chem. Int. Ed.* **1999**, *38*, 1784–1788.
- [20] M. Araki, F. Shima, Y. Yoshikawa, S. Muraoka, Y. Ijiri, Y. Nagahara, T. Shirono, T. Kataoka, A. Tamura, *J. Biol. Chem.* **2011**, *286*, 39644–39653.
- [21] C. Dominguez, R. Boelens, A. M. J. J. Bonvin, *J. Am. Chem. Soc.* **2003**, *125*, 1731–1737.